Wood carbon electrode in microbial fuel cell enhances chromium reduction and bioelectricity generation

Hongyuhang Ni
Lanzhou University
Aman Khan
Lanzhou University
Zi Yang
Lanzhou University
Yuxin Gong
Lanzhou University
Gohar Ali
Lanzhou University
Pu Liu
Lanzhou University
Fengjuan Chen
Lanzhou University
Xiangkai Li (xkli@lzu.edu.cn)
Lanzhou University https://orcid.org/0000-0001-8756-8245

Research Article

Keywords: Wood electrode, MFC, Bioremediation, Electricity generation

Posted Date: April 7th, 2021

DOI: https://doi.org/10.21203/rs.3.rs-317432/v1

Version of Record: A version of this preprint was published at Environmental Science and Pollution Research on September 30th, 2021. See the published version at https://doi.org/10.1007/s11356-021-16652-x.

Abstract

Microbial Fuel Cell (MFC) remediate hexavalent chromium (Cr(VI)) in wastewater, but inefficient removal for wide scale. In this study, a wood carbon (WC) electrode was introduce in MFC to analyzed the Cr(VI) remediation mechanism and effect of WC on it. The results show that the Cr(VI) was completely removed with WC electrode as compare to the carbon cloth (31.12 ± 0.31%) and carbon felt (34.83% ± 0.12) within 48 hours. The maximum power density of the WC electrode was 62.59 ± 0.27 mW m^{-2}. Here in, WC might a good choice with a three-dimensional porous structure for Cr(VI) contaminated wastewater treatment and electricity generation in MFC.

1. Introduction

Hexavalent chromium (Cr(VI)), a toxic metal ion (Saha et al. 2011), comes from electroplating wastewater and causing serious effects on human health (Antoniadis et al. 2018). The reduction of Cr(VI) to (Cr(III)) less toxic by physiochemical treatment have been reported (Avila et al. 2014).. However, these methods are costly, and energy-consuming.

MFC is an effective technique to achieve Cr(VI) reduction as it can be act as an electron acceptor. For instance, MFC with a one-dimensional TiO_2/Fe_2O_3 photoanode could remove 90.9% of Cr(VI) in 13.5 h (Ren et al. 2018). However, the forms of Cr(VI) in MFC will lead to a charge repulsion reaction due to the electrons with negative charge (Wang et al. 2017). Modification of electrodes is a vital method to enhance the usability a of MFC, such as the increment of power generation and organic pollutants reduction (Yellappa et al. 2019).

The development of electrode can assist the reduction of Cr(VI) in MFC. A FeS@rGO modified graphite felt assisted MFC to achieve a 1.43 mg/L/h Cr(VI) deduction (Ali et al. 2019). However, the preparation method of electrodes become limiting factors for the application. It is important to develop electrode materials with good catalytic ability and simple preparation process. Recently, natural biomass has received attention due to inherent porous structure and electrical conductivity properties. For example, kenaf, pomelo peel, and king mushroom have been carbonized under high temperatures and used as the anode of MFC (Chen et al. 2012; Karthikeyan et al. 2015), which can assist MFC to enhanced bioelectricity. The natural carbon materials have strong electrocatalytic ability (Gao et al. 2015), and carbon materials derived from wood would be appropriate to use as an electrode in MFCs.

In this study, wood carbon (WC) electrode was prepared by a simple carbonization process and applied in the cathode of MFC. Optimized the specific surface area and element contents of the electrode at high-temperature. The enhancement of Cr(VI) removal efficiency and bioelectricity generation in MFC due to its dense porous structure and the strong electrocatalytic ability in comparison to control carbon electrodes. Furthermore, surface morphology, electrochemical tests, and valence change of chromium also were conducted in anticipation of using the electrode for practical application.

2. Experimental

2.1. Electrode preparation

Carbon cloth and carbon felt were pretreated (Bond & Lovley 2003), with soaking in 1M NaOH and HCl. To synthesize the wood carbon electrode, basswood (purchased from Chenlin Wood company) was cut into a square and dried at 50°C for 48 h to remove the moisture then calcined at 800°C under N_2 flow for 3 h.

2.2. MFC operation

The MFC was assembled with bottles and divided by PEM. The carbon felt was used as the anode with M_9 media and pre-immobilized bacteria while catholyte media modified (3.0 g/L KH_2PO_4, 0.011 g/L $CaCl_2$, 0.498 g/L $MgSO_4 \cdot 7H_2O$, 17.105 g/L $Na_2HPO_4 \cdot 12H_2O$, 0.5 g/L NaCl, 1.0 g/L NH_4Cl, and 0.1 g/L $NaHCO_3$ at pH 7.0) with a 20 mg/L initial Cr(VI) concentration. A constant temperature (30 °C) was used for operating batch mode.

2.3. Analytical techniques

The polarization curve was obtained by a resistance box (100,000-100 Ω) for the calculation of power density (Heilmann & Logan 2006). Electrochemical measurement includes Tafel plot (TAFEL), A.C. Impedance (IMP), and Cyclic Voltammetry (CV)were performed by potentiostat (CHI604E, Shanghai, China). The IMP test was performed in the frequency range from 1×10^5 to 0.1 Hz with a 10 mV amplitude sinusoidal perturbation. The electrochemical impedance was analyzed according to the Nyquist plots using the ZView software. The Tafel plots ($\ln(j/A) \sim \eta$) were recorded by sweeping overpotential at 1 mVS^{-2} from − 40 to 48 mV.

To analyze residual soluble Cr(VI), samples were filtered and measured by optical density with 1,5-diphenylcarbazide at 540 nm (Omer et al. 2019).

Scanning electron microscopy (SEM, FEI Apreo, Czech) was applied to observe the morphology. The spectrometer (NICOLET, NEXUS 670) was to analyze the functional groups in a wavenumber range of 4000 − 400 cm^{-1}. The specific surface area (SSA) was analyzed from N_2 adsorption-desorption experiment using a micrometric absorber (3 FLEX 3500, USA). Elemental analysis of material was performed on VarioEL Elemental Analyzer (Elementar, Germany). XPS spectra was obtained on an AXIS-ULTRA instrument (Kratos, England), and the results were fitted with software (XPS Peak 41). All graphs and fit curves were made by Graphpad Prism 7 (Graphpad, San Diego, CA, USA).

3. Results And Discussion

3.1. Electrode characterization

A large number of holes were observed on surface of WC by SEM (Fig. 1a & b). The specific surface area of WC was characterized by N_2 adsorption-desorption which was 158.47 $m^2\ g^{-1}$ (Fig. 1c). For functional groups analysis, it showed that 3 stretching vibration modes at 1093, 1622, and 3427 cm^{-1} after high-temperature modification (Fig. 1d). The elemental analysis showed that C and N content reaches 85.34% and 0.52% for WC in comparison with unmodified wood (Table S1).

The performance of WC far exceeding previous materials, such as the carbonized chestnut shell (48.12 $m^2\ g^{-1}$) used in anode MFC (Chen et al. 2016). Due to the stable porosity by 66%, WC electrode has a lower resistivity and increased electron transferability (Jia et al. 2017). Moreover, the modes of FTIR patterns were corresponding to C-O, C = O, and O-H (Mansur et al. 2008) .C group becomes a major after carbonization consistent with FTIR result (Table S1). The increment of C content can enhance the conductivity of WC, whereas the increased N can strengthen electron transfer capacity and promote electrochemical performance of electrodes (Liu et al. 2014). These results suggested that the modification of carbonization can increase porous structure of WC and endow it with better electrochemical activity.

3.2. Cr(VI) reduction in MFC

Cr(VI) was completely reduce by using WC electrode as compare to the carbon felt (34.83% ± 0.12), or carbon cloth (31.12 ± 0.31%) within 48 hrs of incubation in MFC (Fig. 2a). The highest *k* value of WC was (0.08345 ± 0.01 h^{-1}), then carbon cloth (0.007583 ± 0.0005 h^{-1}) and carbon felt (0.007648 ± 0.0005 h^{-1}) (Fig. 2b).

The decrement of WC MFC was more than other MFCs for Cr(VI) reduction, such as carbon cloth (95.28%) with Cu(II) as an electron shuttle mediator, and carbon nano fibers photo cathode modified with cuprous oxide (97%) (Li & Zhou 2019; Pophali et al. 2020). The specific surface area and porous structure of wood electrode promotes Cr(VI)removal efficiency.

3.3 Bioelectricity generation

The carbon felt generate 227 ± 3 mV of voltage was lower than WC electrode 435 ± 2 mV and voltage declines to 75 ± 3 mV later on (Fig. 3a). The highest power density (P_{max}) of WC was 62.59 ± 0.27 mW m^{-2} as compare to the carbon cloth (0.115 ± 0.001 mW m^{-2}) and carbon felt (3.154 ± 0.035 mW m^{-2}) (Fig. 3b). The maximum resistance was 611.3 ± 40.1 Ω of carbon cloth, followed by carbon felt (5.9 ± 0.1 Ω) and WC electrode (0.9 ± 0.01 Ω) (Fig. 3c, d).

The voltage output was higher than previously reported results for the traditional MFC with graphene modified graphite felt cathode (411 ± 12 mV) (Song et al. 2016). The maximum power density was (55.5 mW m^{-2}) that *Trichococcus pasteurii* and *Pseudomonas aeruginosa* were functioned as biocatalysts (Tandukar et al. 2009). The data indicates that WC electrodes not only enhance electron transfer but also increase power output.

3.4. Electrochemical characteristics

The CV patterns indicated that cathodes have a reduction peak at 0.235 V, 0.401 V, and 0.443 V (vs Ag/AgCl) for carbon cloth, carbon felt, and WC, respectively (Fig. 4a). Tafel plots have exhibited the exchange current densities between electrodes and electrons acceptor (Fig. 4b). The values of the reductive Tafel slop were 277.3, 139.8, and 110.5 V dec^{-1}, for the carbon cloth, carbon felt, and WC (Fig. 4c). EIS was performed to analyze the impedance of three different cathodes (Fig. 4d). WC showed t low charge transfer resistance (0.42 ± 0.01 Ω) compared to the carbon cloth (43.77 ± 7.67 Ω) and carbon felt (201.3 ± 31.9 Ω) electrodes (Fig. 4e).

The oxidation-reduction loop areas were different from each other, which reveals electrons transfer capacity best at WC surface. The electro-active ability could be defined by stoichiometry (Tafel plots), where the ability is inversely proportional to slop values. The low resistance of wood electrode indicates better and faster charge transferability on the surface. A significant reduction of R_{ct} to the porous structure of wood improved the interfacial interaction between the electron acceptor and electrode surface. Hence WC cathode has an strong absorption ability to reduce Cr(VI).

3.5. Mechanism of Cr(VI) reduction

No apparent signal of Cr(VI) was observed in carbon cloth from XPS pattern (Fig. S1), due to the limited adsorption capacity. However, the peaks of Cr appeared on the WC cathode at the binding energy of 574.3 and 584.7 eV (Fig. S1c, d), showed deposition of chromium on surface. One characteristic peaks of oxygen appeared on the WC at 529.2 eV (Fig. S1)

The binding energy of chromium peaks was corresponding to Cr(III) (Crist & Crisst 2000). Cr(VI) absorption of WC was stronger than carbon cloth and Cr(VI) can be reduced to Cr(III) precipitated substances (Cr_2O_3 or $Cr(OH)_3$). In addition, the binding energy peak of Oxygen (O 1S) corresponded to O1 peak, which represented the metal-O band (Cheng et al. 2019). Therefore, above results proved that WC electrode absorb chromium ions, reduce them to Cr_2O_3, and then deposit on the surface of the wood:

$$Cr_2O_7^{2-} + 14H^+ + 6e^- \rightarrow 2Cr^{3+} + 7H_2O^+$$

The cost of WC electrode was evaluated with previous electrodes. The preparation cost of it is about 0.00085 $/piece, far lower than the traditional graphene felt (0.114 $/piece) (Table S2) (Guo et al. 2016; Li et al. 2018). Therefore, the availability of WC electrode in MFC enhanced Cr(VI) removal efficiency

4. Conclusions

A mesoporous, three-dimensional WC could utilized for efficient Cr(VI) removal and bioelectricity generation in MFC. WC electrode can achieve high power density with 100% of Cr(VI) removal which was 18.87 and 1.87 times higher than carbon felt. The mechanism of the Cr(VI) removal efficiency and power

output were ascribed to the advanced electrocatalytic effect and microstructure with partially-aligned and irregular channels after a high temperature modification. It has been recommended, WC novel electrode has great prospects for heavy metals contaminated water treatment in future.

Declarations

Funding; This work was supported by National Natural Science Foundation Grant (No: 31870082 & 21876072); Gansu province major science and technology projects (No: 17ZD2WA017); Fundamental Research Funds for the Central Universities (No: lzujbky-2020-83); Chengguan District Science and Technology Development Project (No: 2020JSCX0019); Gansu province international cooperation funds (No: 1504WKCA089-2).

Conflicts of interest; The authors declare that they have no known competing financial interests.

Ethics approval; Not applicable

Consent to participate; Not applicable

Consent for publication; Not applicable

Availability of data and material; Not applicable

Code availability; Not applicable

Authors contribution Hongyuhang Ni: Conceptualization, Methodology, Software, Formal analysis, Date curation, Writing-original draft, Wring-review & editing; **Zi Yang:** Methodology, Formal analysis, Resources, Writing-original Draft; **Aman khan:** Investigation, Date curation, Writing-original draft; **Yuxin Gong:** Formal analysis; **Gohar Ali:** Writing-original draft; **Pu Liu:** Writing-original draft; **Fengjuan Chen:** Conceptualization, Resources, Supervision; **Xiangkai Li:** Conceptualization, Date curation, Supervision, Project administration.

References

Ali J, Wang L, Waseem H, Djellabi R, Oladoja N, Pan G (2019). FeS@ rGO nanocomposites as electrocatalysts for enhanced chromium removal and clean energy generation by microbial fuel cell. Chemical Engineering Journal: 123335

Antoniadis V, Zanni A A, Levizou E, Shaheen S M, Dimirkou A, Bolan N, Rinklebe J (2018). Modulation of hexavalent chromium toxicity on Omicronriganum vulgare in an acidic soil amended with peat, lime, and zeolite. Chemosphere 195: 291-300. https://doi.org/10.1016/j.chemosphere.2017.12.069.

Avila M, Burks T, Akhtar F, Göthelid M, Lansåker P C, Toprak M S, Muhammed M, Uheida A (2014). Surface functionalized nanofibers for the removal of chromium(VI) from aqueous solutions. Chemical

Engineering Journal 245: 201-209. https://doi.org/10.1016/j.cej.2014.02.034.

Bond D R, Lovley D R (2003). Electricity Production by Geobacter sulfurreducens Attached to Electrodes. Applied and Environmental Microbiology 69(3): 1548-1555. https://doi.org/10.1128/aem.69.3.1548-1555.2003.

Chen S, He G, Hu X, Xie M, Wang S, Zeng D, Hou H, Schroder U (2012). A three-dimensionally ordered macroporous carbon derived from a natural resource as anode for microbial bioelectrochemical systems. ChemSusChem 5(6): 1059-63. https://doi.org/10.1002/cssc.201100783.

Chen S, Tang J, Jing X, Liu Y, Yuan Y, Zhou S (2016). A hierarchically structured urchin-like anode derived from chestnut shells for microbial energy harvesting. Electrochimica Acta 212: 883-889. https://doi.org/10.1016/j.electacta.2016.07.077.

Cheng C, Hu Y, Shao S, Yu J, Zhou W, Cheng J, Chen Y, Chen S, Chen J, Zhang L (2019). Simultaneous Cr(VI) reduction and electricity generation in Plant-Sediment Microbial Fuel Cells (P-SMFCs): Synthesis of non-bonding Co3O4 nanowires onto cathodes. Environmental Pollution 247: 647-657. https://doi.org/10.1016/j.envpol.2019.01.084.

Crist B V, Crisst D B. 2000. *Handbook of monochromatic XPS spectra*. Wiley New York.

Gao S, Wei X, Fan H, Li L, Geng K, Wang J (2015). Nitrogen-doped carbon shell structure derived from natural leaves as a potential catalyst for oxygen reduction reaction. Nano Energy 13: 518-526

Guo K, Hidalgo D, Tommasi T, Rabaey K (2016). Pyrolytic carbon-coated stainless steel felt as a high-performance anode for bioelectrochemical systems. Bioresour Technol 211: 664-8. https://doi.org/10.1016/j.biortech.2016.03.161.

Heilmann J, Logan B E (2006). Production of Electricity from Proteins Using a Microbial Fuel Cell. Water Environment Research 78(5): 531-537. https://doi.org/10.2175/106143005x73046.

Jia C, Li Y, Yang Z, Chen G, Yao Y, Jiang F, Kuang Y, Pastel G, Xie H, Yang B, Das S, Hu L (2017). Rich Mesostructures Derived from Natural Woods for Solar Steam Generation. Joule 1(3): 588-599. https://doi.org/10.1016/j.joule.2017.09.011.

Karthikeyan R, Wang B, Xuan J, Wong J W C, Lee P K H, Leung M K H (2015). Interfacial electron transfer and bioelectrocatalysis of carbonized plant material as effective anode of microbial fuel cell. Electrochimica Acta 157: 314-323. https://doi.org/10.1016/j.electacta.2015.01.029.

Li M, Zhou S (2019). Efficacy of Cu (II) as an electron-shuttle mediator for improved bioelectricity generation and Cr (VI) reduction in microbial fuel cells. Bioresource technology 273: 122-129

Li T, Song J, Zhao X, Yang Z, Pastel G, Xu S, Jia C, Dai J, Chen C, Gong A (2018). Anisotropic, lightweight, strong, and super thermally insulating nanowood with naturally aligned nanocellulose. Science advances

4(3): eaar3724

Liu J, Liu J, He W, Qu Y, Ren N, Feng Y (2014). Enhanced electricity generation for microbial fuel cell by using electrochemical oxidation to modify carbon cloth anode. Journal of Power Sources 265: 391-396. https://doi.org/10.1016/j.jpowsour.2014.04.005.

Mansur H S, Sadahira C M, Souza A N, Mansur A A P (2008). FTIR spectroscopy characterization of poly (vinyl alcohol) hydrogel with different hydrolysis degree and chemically crosslinked with glutaraldehyde. Materials Science and Engineering: C 28(4): 539-548. https://doi.org/10.1016/j.msec.2007.10.088.

Omer A M, Khalifa R E, Hu Z, Zhang H, Liu C, Ouyang X K (2019). Fabrication of tetraethylenepentamine functionalized alginate beads for adsorptive removal of Cr (VI) from aqueous solutions. Int J Biol Macromol 125: 1221-1231. https://doi.org/10.1016/j.ijbiomac.2018.09.097.

Pophali A, Singh S, Verma N (2020). A dual photoelectrode-based double-chambered microbial fuel cell applied for simultaneous COD and Cr (VI) reduction in wastewater. International Journal of Hydrogen Energy

Ren G, Sun Y, Lu A, Li Y, Ding H (2018). Boosting electricity generation and Cr(VI) reduction based on a novel silicon solar cell coupled double-anode (photoanode/bioanode) microbial fuel cell. Journal of Power Sources 408: 46-50. https://doi.org/10.1016/j.jpowsour.2018.10.081.

Saha R, Nandi R, Saha B (2011). Sources and toxicity of hexavalent chromium. Journal of Coordination Chemistry 64(10): 1782-1806. https://doi.org/10.1080/00958972.2011.583646.

Song T S, Jin Y, Bao J, Kang D, Xie J (2016). Graphene/biofilm composites for enhancement of hexavalent chromium reduction and electricity production in a biocathode microbial fuel cell. J Hazard Mater 317: 73-80. https://doi.org/10.1016/j.jhazmat.2016.05.055.

Tandukar M, Huber S J, Onodera T, Pavlostathis S G (2009). Biological chromium(VI) reduction in the cathode of a microbial fuel cell. Environmental Science & Technology 43(21): 8159-8165

Wang Q, Huang L, Pan Y, Quan X, Li Puma G (2017). Impact of Fe(III) as an effective electron-shuttle mediator for enhanced Cr(VI) reduction in microbial fuel cells: Reduction of diffusional resistances and cathode overpotentials. Journal of Hazardous Materials 321: 896-906. https://doi.org/10.1016/j.jhazmat.2016.10.011.

Yellappa M, Sravan J S, Sarkar O, Reddy Y V R, Mohan S V (2019). Modified conductive polyaniline-carbon nanotube composite electrodes for bioelectricity generation and waste remediation. Bioresour Technol 284: 148-154. https://doi.org/10.1016/j.biortech.2019.03.085.

Figures

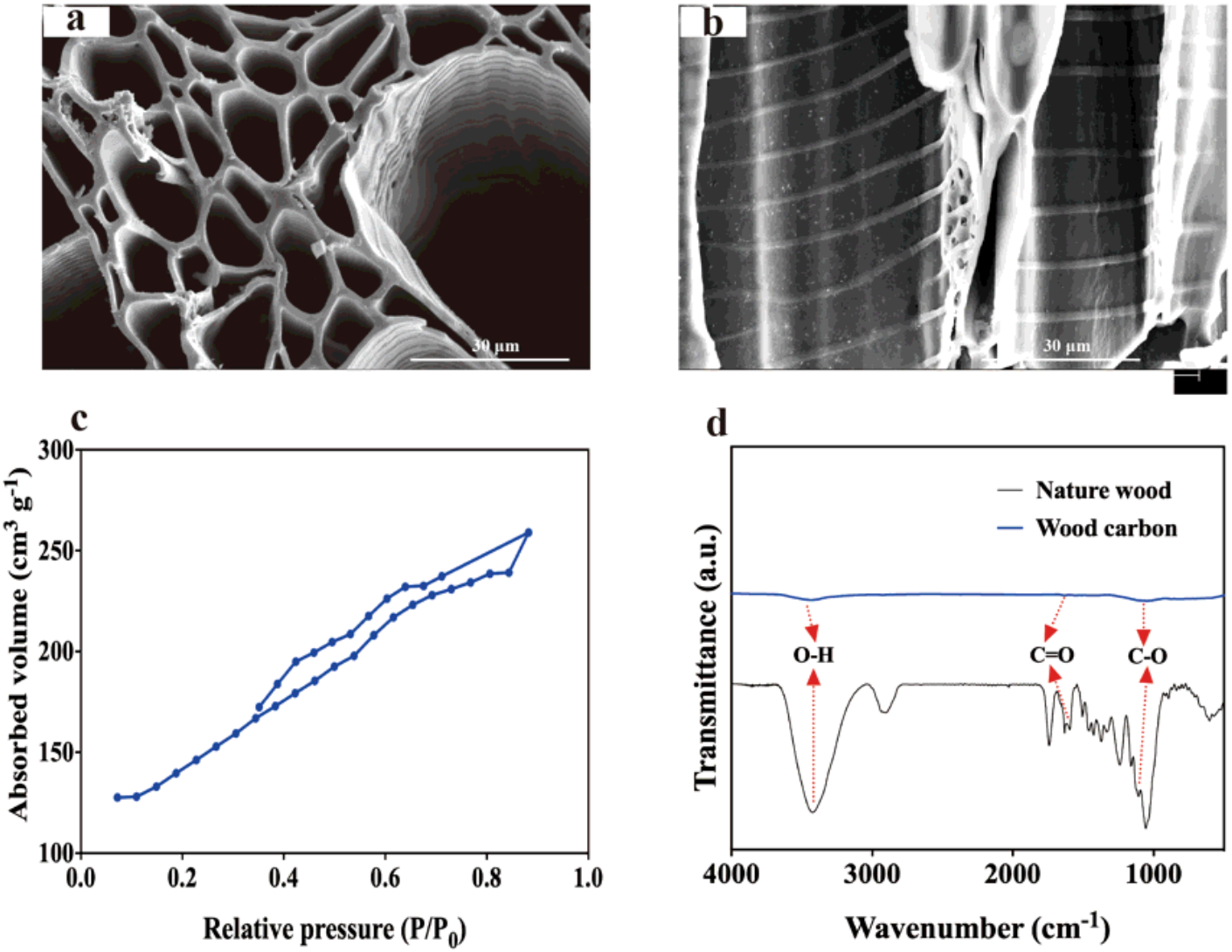

Figure 1

Characterization of WC electrode, (a) surface in cross-section, (b) surface in longitude-section, (c) nitrogen absorption/desorption isotherm, (d) Fourier transform infrared spectroscopy (FTIR) spectra of WC and natural wood.

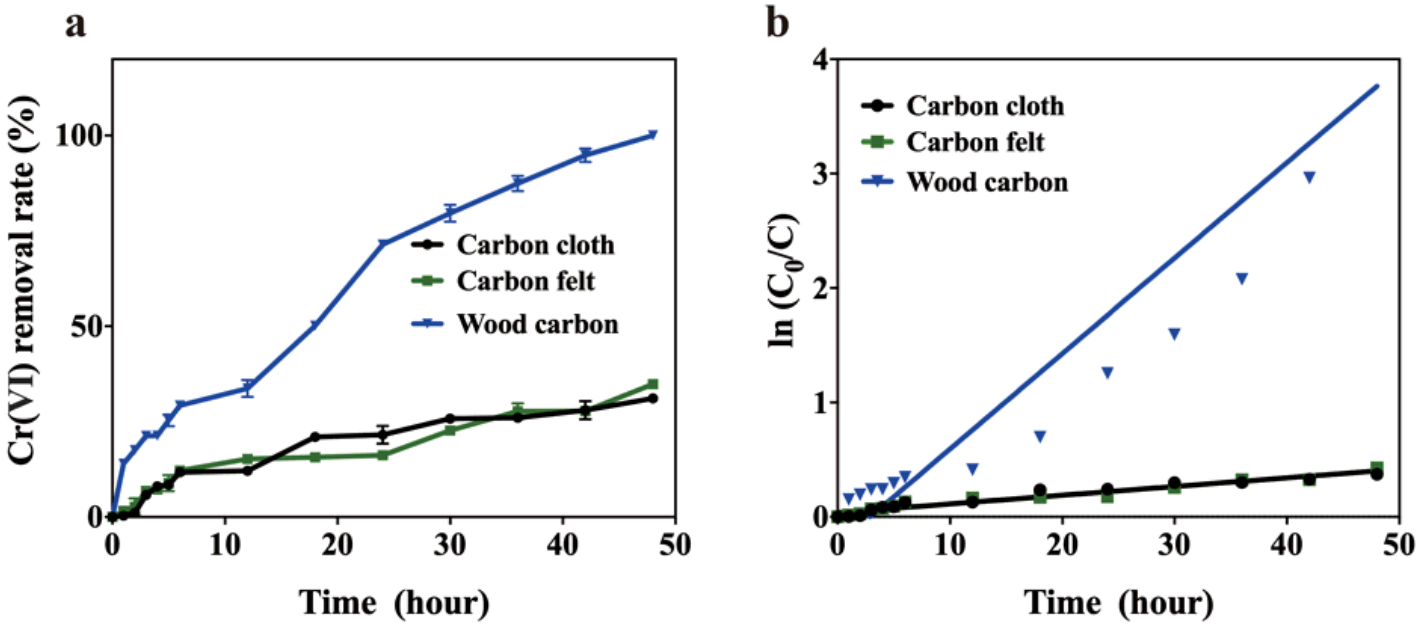

Figure 2

Time course of Cr(VI) removal efficiency in the chamber of MFCs. (a) the close-circuit condition and (b) ln (C0/C) in 48 hours

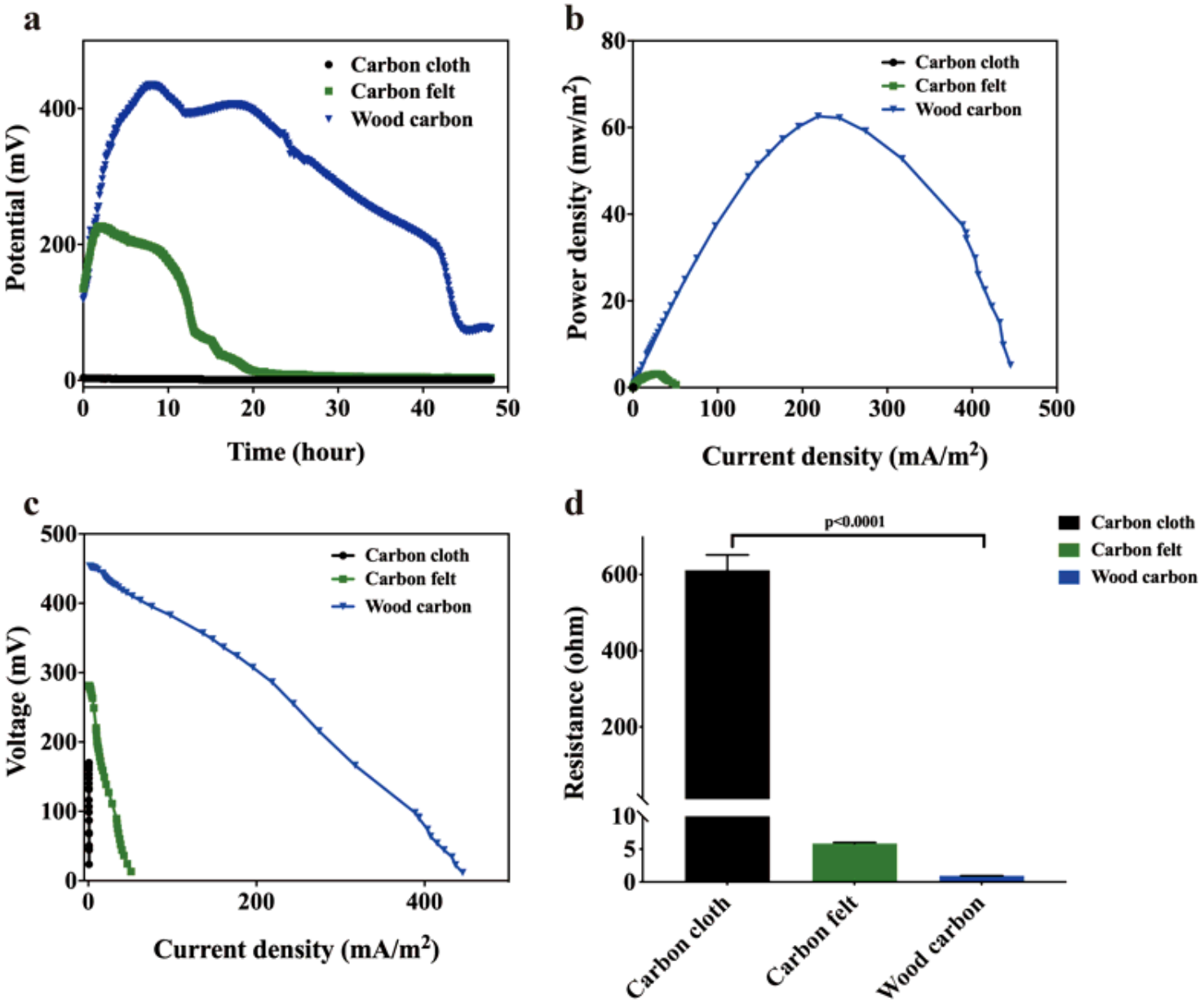

Figure 3

Bioelectricity generation performance of MFC. (a) Voltage outputs, (b) power density, (c) polarization curves and (d) internal resistance of MFC with different cathodes.

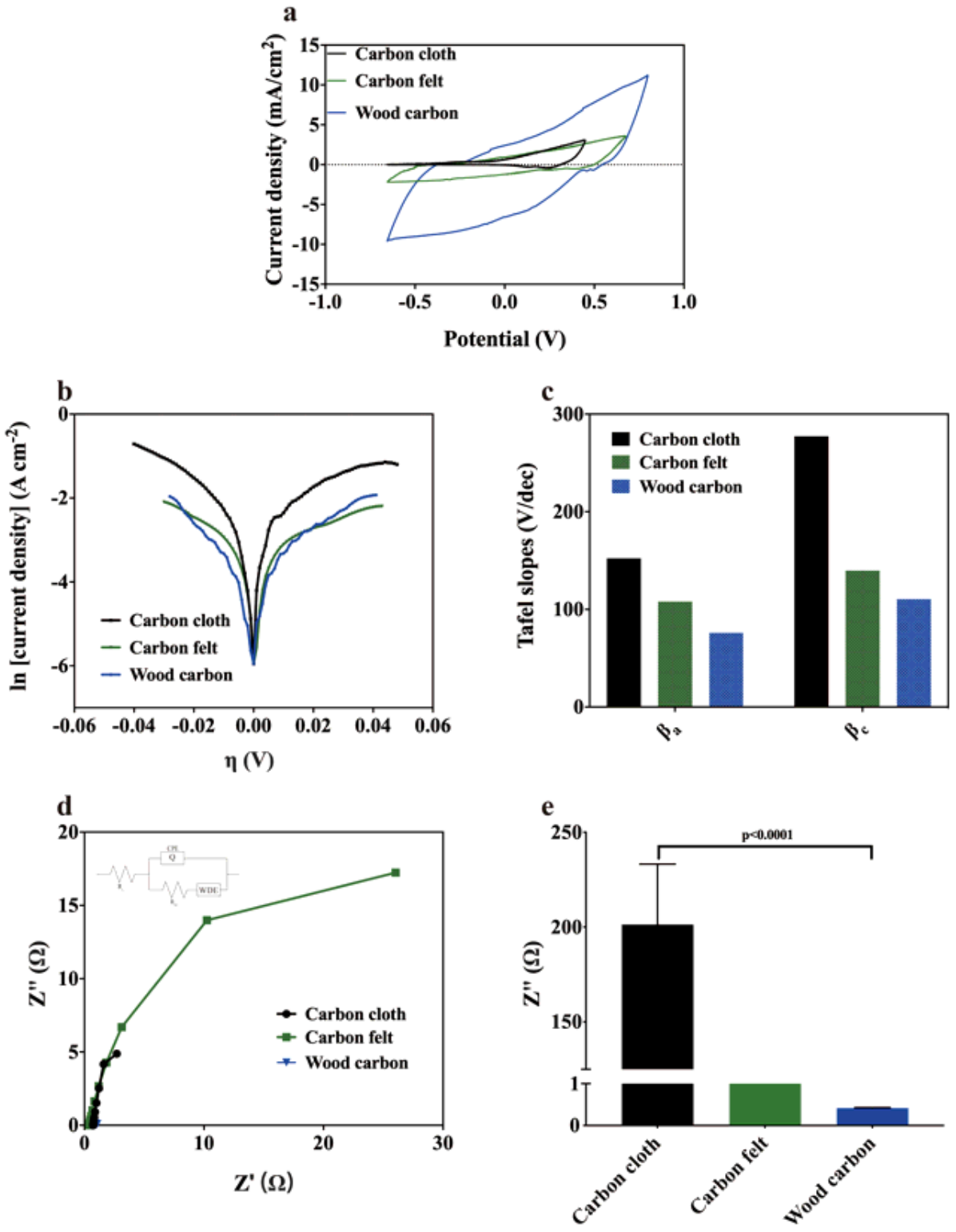

Figure 4

Electrochemical activities of cathodes (a) Cyclic voltammogram curves (b) Tafel plots; (c) the values of Tafel slop; (d) Nyquist plots of different electrodes (Inset: equivalent circuit model) and (e) comparison among different electrodes in charge transfer resistance.

Supplementary Files

This is a list of supplementary files associated with this preprint. Click to download.

- SupplementaryInformation.docx